Implementation of helical wave propagation motion in snake robot moving on exterior of a pipe

Wei Qi*

Graduate School of Natural Science and Technology,
Okayama University,
Okayama-shi, Okayama, Japan
Email: qi.w.mif@s.okayama-u.ac.jp
*Corresponding author

Tetsushi Kamegawa and Akio Gofuku

Graduate School of Interdisciplinary Science and Engineering in Health Systems,
Okayama University,
Okayama-shi, Okayama, Japan
Email: kamegawa@okayama-u.ac.jp
Email: gofuku-a@okayama-u.ac.jp

Abstract: In this study, we developed a snake robot that goes through a branch point on exterior of a pipe in a helical shape. A hyperbolic function is utilised to generate a wave along the helical curve. The joint angles of the snake robot are derived by calculating the curvature and torsion of the curve by using the formula of the continuous curve model. We implemented the new motion in a real snake robot by considering parameters of the curve. In addition, we propose a method to compensate for the effect of gravity to achieve the motion by a real snake robot. Experimental results are shown to validate the effectiveness of the proposed method.

Keywords: snake robot; helical wave propagation motion; hyperbolic function; pipe with branch.

Reference to this paper should be made as follows: Qi, W., Kamegawa, T. and Gofuku, A. (2017) 'Implementation of helical wave propagation motion in snake robot moving on exterior of a pipe', *Int. J. Advanced Mechatronic Systems*, Vol. 7, No. 6, pp.359–367.

Biographical notes: Wei Qi received his MS degree from the Graduate School of Natural Science and Technology, Okayama University, Okayama, Japan, in 2014. In the same year, he worked at the College of Mechanical Engineering, Inner Mongolia University for Nationalities, China, as a Teaching Assistant. Currently, he is a PhD student at the Graduate School of Natural Science and Technology, Okayama University. His research focuses on designing a new way of movement for a snake robot. He is a student member of the JSME.

Tetsushi Kamegawa received his BS, MS and PhD degrees in Engineering from Tokyo Institute of Technology, Japan, in 1999, 2001 and 2004, respectively. In 2004, he was a Visiting Scholar of Roma University, Italy. From 2004 to 2006, he was a Researcher at International Rescue System Institute, Japan. From 2006 to 2009, he worked as a Research Associate, Assistant Professor and Senior Assistant Professor at the Okayama University, Japan. His research interests include snake robots, rescue robot and medical robot. He is a member of the JSME, RSJ and SICE.

Akio Gofuku received his BS, MS and PhD degrees in Engineering from Kyoto University, Japan, in 1981, 1983 and 1990, respectively. He was a Research Associate of the Institute of Atomic Energy, Kyoto University from April 1984 to November 1994. From September 1993 to August 1994, he was a Visiting Researcher of Technical University of Denmark, Denmark. He moved Okayama University, Japan as an Associate Professor in December, 1994 and currently he is a Professor of the Graduate School of Interdisciplinary Science and Engineering in Health Systems, Okayama University. His research interests include human-machine interface of industrial plants, spherical motor and medical support systems. He is a member of the AESJ, JSME, HIS, JSAI, JSAEM, and so on.

1 Introduction

Although the form of a biological snake is simple, snakes can move in various environments by using several methods. They can grip an object by wrapping around it as well as move along it. It is considered that the development of a snake robot that mimics the characteristics of a biological snake have significant advantages because it can perform various tasks although it is a simple form. For example, snake robots would be utilised in the field of pipe inspection, and small size of snake robots would be suitable for in-vivo applications like a capsule robot (Liu et al., 2018). Thus far, several types of mechanisms and controllers for snake robots have been studied. Hirose et al. revealed the principle of the undulatory curve of a biological snake and called it a serpenoid curve (Hirose, 1993; Hirose and Yamada, 2009; Mori and Hirose, 2001). Moreover, based on the finding that biological snakes are propelled by frictional differences between the tangential and normal directions on their trunk, a smooth, undulatory snake robot motion with passive wheels has been realised (Hirose, 1993; Mori and Hirose, 2001). To extend the configuration space of snake robots to three-dimensional (3D) space, snake robots constructed by alternately combining pitch and yaw axes have been developed. By using these robots, various motions, such as sidewinding, lateral rolling, and helical rolling, have been realised (Kamegawa et al., 2002; Date and Takita, 2005; Rollinson and Choset, 2016). Sidewinding motion has been observed as the method of locomotion of snakes in a desert when they move across loose or slippery environments. Lateral rolling and helical rolling motions are rarely seen in biological snakes; thus, these motions are considered unique snake robot motions. Specifically, helical rolling motion has been used to help snake robots move along the interior or exterior of a pipe (Kamegawa et al., 2009; Baba et al., 2010; Lipkin et al., 2007; Rollinson and Choset, 2016). This type of motion allows for movement along a pipe by twisting the trunk of a snake robot in a state of coiling around a pipe. However, this motion is unsuitable if there is a branch on the pipe when moving along the exterior of a pipe; in that case, the snake robot can no longer move forward across the branch.

In previous research, we proposed a new motion of a snake robot that wraps around the exterior of a pipe and overcomes a branch point on the pipe. The new motion is called helical wave propagation motion (Qi et al., 2017). This motion is also unique to snake robots. A helical wave curve is propagated by shifting the shape of the hyperbolic function. To our knowledge, this is a new method for moving a snake robot along the direction tangential to its body. However, the motion was not implemented to a real snake robot yet.

In this paper, we give a guide to determine the parameter settings for a real snake robot and show results of the experiment by using a real snake robot. In addition, when implementing the new motion in a real snake robot, it is necessary to compensate for the effect of gravity. We propose a method to compensate for gravity, which involves overlaying additional twisting at the point where the helical wave curve is applied. The effectiveness of the motion is verified by experiments conducted using a real snake robot.

2 Helical rolling motion based on continuous curve model

When planning the motion of a snake robot, a method that uses the curvature and torsion of the snake's trunk (expressed as a continuous curve model) is often used. The target joint angles for snake robots based on a continuous curve model have been derived in previous publications (Yamada and Hirose, 2006, 2010). The target angles of the snake robot joints are applied to a mechanical system to realise the planned motion. An outline of the method for helical rolling motion is described below. The helix is a basic shape for achieving helical wave propagation motion, as will be described in this section.

2.1 Mathematical continuum model

A continuum curve in 3D space is expressed using the Frenet-Serret equation, which expresses a curve $\mathbf{c}(s)$ by using curvature $\kappa(s)$ and torsion $\tau(s)$.

$$\begin{cases} d\mathbf{c}(s)/ds = \mathbf{e_1}(s) \\ d\mathbf{e_1}(s)/ds = \kappa(s)\mathbf{e_2}(s) \\ d\mathbf{e_2}(s)/ds = -\kappa(s)\mathbf{e_1}(s) + \tau(s)\mathbf{e_3}(s) \\ d\mathbf{e_3}(s)/ds = -\tau(s)\mathbf{e_2}(s) \end{cases} \tag{1}$$

where s is a parameter of length along the curve. $\mathbf{e_1}(s)$, $\mathbf{e_2}(s)$, and $\mathbf{e_3}(s)$ are orthonormal basis unit vectors. $\mathbf{e_1}(s)$ is a vector tangential to the curve at s, $\mathbf{e_2}(s)$ is a vector that indicates the direction of change of the curve at s and $\mathbf{e_3}(s)$ is a vector given by $\mathbf{e_3}(s) = \mathbf{e_1}(s) \times \mathbf{e_2}(s)$ as shown in Figure 1.

However, the Frenet-Serret formulation is not suitable for a snake robot's coordinate system because it only gives the shape of the curved line, whereas a snake robot's coordinate system should correspond to the joint structure of the robot. By considering the fact that a mechanical snake robot's coordinate system $\mathbf{e_r}(s)$, $\mathbf{e_p}(s)$, $\mathbf{e_y}(s)$ is introduced, as shown in Figure 2, let $\tau_{roll}(s)$, $\kappa_{pitch}(s)$, and $\kappa_{yaw}(s)$ be torsion of roll, curvature of pitch, and curvature of yaw at point s on the continuum robot's coordinate system, respectively. In this formulation, the continuum curve is given by the following equations:

$$\begin{cases} d\mathbf{c}(s)/ds = \mathbf{e_r}(s) \\ d\mathbf{e_r}(s)/ds = \kappa_{yaw}(s)\mathbf{e_p}(s) - \kappa_{pitch}(s)\mathbf{e_y}(s) \\ d\mathbf{e_p}(s)/ds = -\kappa_{yaw}(s)\mathbf{e_r}(s) + \tau_{roll}(s)\mathbf{e_y}(s) \\ d\mathbf{e_y}(s)/ds = \kappa_{pitch}(s)\mathbf{e_r}(s) - \tau_{roll}(s)\mathbf{e_p}(s) \end{cases} \tag{2}$$

$\tau_{roll}(s)$, $\kappa_{pitch}(s)$ and $\kappa_{yaw}(s)$ determine the shape of the continuum curve in 3D space.

Figure 1 Coordinate system of Frenet-Serret formulation (see online version for colours)

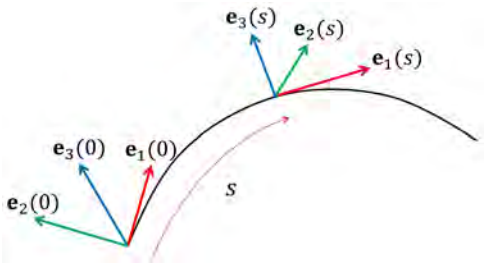

Figure 2 Illustration of coordinate system for snake robot (see online version for colours)

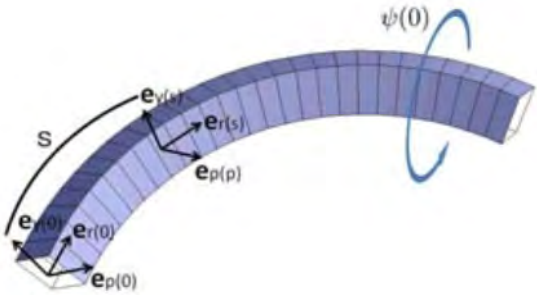

Figure 3 $\psi(s)$: difference of angle between $\mathbf{e}_2(s)$ and $\mathbf{e}_p(s)$ (see online version for colours)

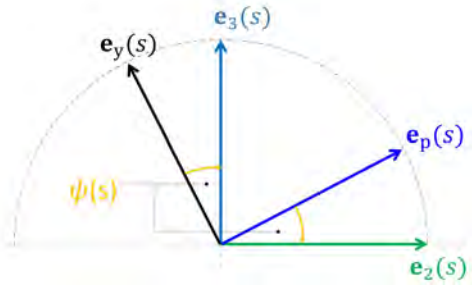

The snake robot in this paper has only pitch and yaw axes. There is no roll axis. Therefore, $\tau_{roll}(s)$ in equation (2) is 0. Equation (2) then becomes the following:

$$\begin{cases} d\mathbf{c}(s)/ds = \mathbf{e}_r(s) \\ d\mathbf{e}_r(s)/ds = \kappa_{yaw}(s)\mathbf{e}_p(s) - \kappa_{pitch}(s)\mathbf{e}_y(s) \\ d\mathbf{e}_p(s)/ds = -\kappa_{yaw}(s)\mathbf{e}_r(s) \\ d\mathbf{e}_y(s)/ds = \kappa_{pitch}(s)\mathbf{e}_r(s) \end{cases} \tag{3}$$

Let $\psi(s)$ be the angular difference between $\mathbf{e}_2(s)$ and $\mathbf{e}_p(s)$, as shown in Figure 3.

$$\begin{cases} \mathbf{e}_p(s) = \mathbf{e}_2(s)\cos\psi(s) - \mathbf{e}_3\sin\psi(s) \\ \mathbf{e}_y(s) = \mathbf{e}_2(s)\sin\psi(s) + \mathbf{e}_3\cos\psi(s) \end{cases} \tag{4}$$

$\kappa_{yaw}(s)$ and $\kappa_{pitch}(s)$ in equation (3) are expressed using $\kappa(s)$ and $\tau(s)$ as follows.

$$\begin{cases} \kappa_{pitch}(s) = -\kappa(s)\sin(\psi(s)) \\ \kappa_{yaw}(s) = \kappa(s)\cos(\psi(s)) \\ \psi(s) = \int_0^s \tau(s)ds + \psi(0) \end{cases} \tag{5}$$

where $\psi(0)$ is an integral constant value at time t, and it can be decided arbitrarily by an operator to generate rolling motion.

2.2 Design of helical shape and rolling motion

The helical shape is expressed as follows in Cartesian coordinates.

$$\begin{cases} x(t) = a\cos(t) \\ y(t) = a\sin(t) \\ z(t) = b(t) \end{cases} \tag{6}$$

where a denotes the helical radius, b is the increase ratio of the helical shape along the z direction, and t is a parameter. An example of a helical shape generated using equation (6) is shown in Figure 4.

Figure 4 Example of helical shape (a = 0.2, b = 0.05) (see online version for colours)

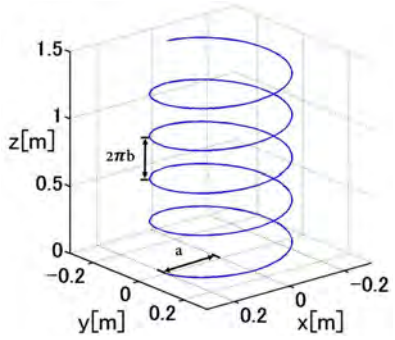

After designing the helical shape in the Cartesian coordinate system, the target shape was converted to a curve by using the Frenet-Serret formulation. The curvature and torsion of the curve were obtained using the geometrical conditions given by the following equations:

$$\kappa(t) = \frac{\sqrt{(\dot{y}\ddot{z} - \dot{z}\ddot{y})^2 + (\dot{z}\ddot{x} - \dot{x}\ddot{z})^2 + (\dot{x}\ddot{y} - \dot{y}\ddot{x})^2}}{\left(\dot{x}^2 + \dot{y}^2 + \dot{z}^2\right)^{\frac{3}{2}}} \tag{7}$$

$$\tau(t) = \frac{x^{(3)}(\dot{y}\ddot{z} - \dot{z}\ddot{y}) + y^{(3)}(\dot{z}\ddot{x} + \dot{x}\ddot{z}) + z^{(3)}(\dot{x}\ddot{y} + \dot{y}\ddot{x})}{(\dot{y}\ddot{z} - \dot{z}\ddot{y})^2 + (\dot{z}\ddot{x} - \dot{x}\ddot{z})^2 + (\dot{x}\ddot{y} + \dot{y}\ddot{x})^2} \tag{8}$$

where, $\dot{x}$, $\ddot{x}$ and $x^{(3)}$ denote first-, second- and third-order differentiation with respect to t, respectively. Note that the parameter t in equations (7) and (8) should convert to parameter s when κ and τ are applied to the Frenet-Serret formulation in equation (1).

By substituting equation (6) into equations (7) and (8), we obtain the curvature and torsion, respectively, as follows:

$$\kappa(t) = \frac{a}{a^2 + b^2} \tag{9}$$

$$\tau(t) = \frac{b}{a^2 + b^2} \tag{10}$$

By changing the values of a and b in equations (6), the radius and pitch of the helical shape can be designed. Furthermore, by changing the value of $\psi(0)$, the coordinate system of the continuum robot is rolled around $\mathbf{e_r}(s)$ such that the robot generates a lateral rolling motion.

2.3 Application to discrete mechanical snake robot model

According to the definition of curvature, the degrees of relative rotation of the pitch and yaw joints of the robot's coordinate system can be expressed as $\kappa_{pitch}(s)ds$ and $\kappa_{yaw}(s)ds$, respectively. Therefore, if the length between the pitch and yaw joints of a discrete mechanical snake robot is δ_s, the desired angle of the i^{th} joint θ_i^d can be obtained as follows:

$$\theta_i^d = \begin{cases} 2\delta s \cdot \kappa_{yaw}(i\delta s)\ (i:\text{odd joint}) \\ 2\delta s \cdot \kappa_{pitch}(i\delta s)\ (i:\text{even joint}) \end{cases} \tag{11}$$

In this study, odd-numbered joints are yaw joints, and even-numbered joints are pitch joints. The coefficient '2' indicates that the interval of the pitch or yaw joints is $2\delta s$.

Figure 5 Illustration of helical rolling motion: $s = l$ is the head of the snake robot and $s = 0$ is the tail of the snake robot; B is the binormal direction, and T is the direction tangential to the snake robot's body, (a) state of a snake robot climbing a pipe through helical rolling motion (b) the state is projected in the z-$r\theta$ plane; on this plane, the shape of the snake robot is a line (see online version for colours)

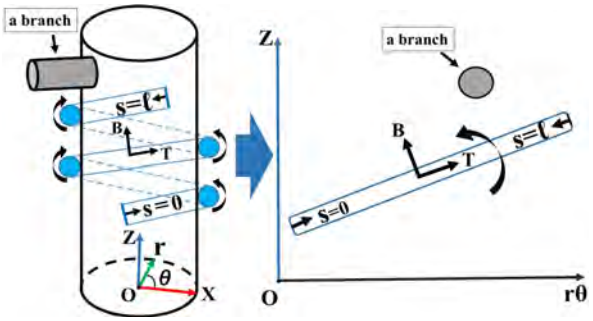

(a) (b)

2.4 Problems associated with helical rolling motion

The helical rolling motion helps a snake robot move along a pipe by twisting its trunk in a state of coiling around the pipe. Snake robots can move along cylindrical objects by using helical rolling motion. Although there are a few research reports on the movement along a pipe by means of helical rolling motion, several challenges related to this type of motion remain. Especially, a snake robot cannot overcome the part of a pipe that contains a branch point, as shown in Figure 5. The snake robot never crosses a branch point so long as it moves along a binormal direction with respect to its body. To address this challenge, we consider making the snake robot move in a direction tangential to its body, as shown in Figure 6, as opposed to a binormal direction, by means of helical rolling motion.

Figure 6 Helical wave propagation on z-$r\theta$ plane (see online version for colours)

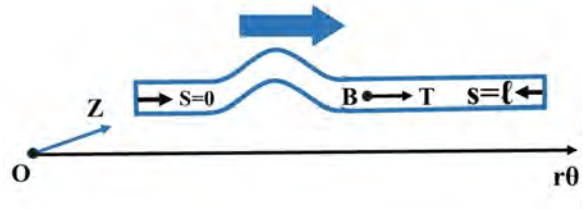

3 Formulation of helical wave curves

3.1 Design of helical wave curve

At first, it is assumed that a snake robot is wrapped around a pipe. Thereafter, it generates a longitudinal wave by lifting parts of its trunk from the surface of the pipe. The floating parts are transmitted from the tail to the head of the snake robot by using the shifting method (Qi et al., 2017). In the present study, the helical wave curve is expressed in Cartesian coordinates as follows:

$$\begin{cases} x(t) = a(t)\cos(t) \\ y(t) = a(t)\sin(t) \\ z(t) = b(t) \end{cases} \tag{12}$$

where

$$a(t) = \rho(t) + r$$
$$b(t) = \frac{n}{2\pi}t \tag{13}$$

$$\rho(t) = A\,\text{sech}\,(\omega t - \phi)$$
$$\{A \in \mathcal{R} \mid A > 0\}, \{\omega \in \mathcal{R} \mid \omega > 0\}, \phi \in \mathcal{R} \tag{14}$$

where r is the radius of the helical curve, n is the pitch along the z-axis of the helical curve, and t is a parameter. It is very important to find an appropriate $a(t)$ to add an appropriate wave to an ordinary helical curve. We designed $a(t)$ as a hyperbolic function of *sech* added to the radius r. In equation (14), A is the amplitude, ω is width of the curve, and ϕ is initial phase of helical wave curve. As shown in Figure 7, we can design the hyperbolic function by changing these parameters.

Next, the experimental parameters of the snake robot were determined. According to equations (12) and (13), a snake robot forms a helical curve of radius r. r is composed of the robot's trunk radius r_r and the pipe radius r_p.

$$r = r_r + r_p \tag{15}$$

n is the pitch of the helical curve along the z-axis, and it is determined by the width of a branch point w_b and the diameter of the robot trunk $2r_r$.

$$2\pi n \geq w_b + 2r_r \tag{16}$$

Figure 7 Example of hyperbolic function of sech in the domain $[-2\pi, 2\pi]$ ($A = 0.01$, $\omega = 1$, $\phi = 0$) (see online version for colours)

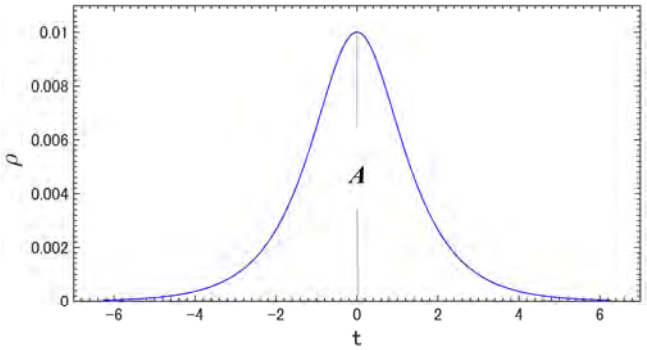

In the case of helical wave curve, the radius of the helical curve changes from r to $r + A$. $r + A$ is a peak of the helical wave curve. By contrast, ω is the width of the helical wave curve. The abscissas of the curve decrease $1/\omega$ times if ω is increased. Note that the values of A and ω can influence the curvature and torsion of the helical wave curve. It is important to check curvature and torsion to realise the motion by a real snake robot because they directly relate to the joint angle of the robot. From Figures 8 and 9, when $\omega = 1$, the curvature and torsion change gently, and they do not exceed the value of curvature and torsion of the helical curve. The curvature and torsion are about $\kappa = 10.8$, $\tau = 0.54$ in Figures 8 and 9. By contrast, as ω increases, the curvature and torsion change substantially, and they exceed the values of curvature and torsion of the helical curve. In this case, the servomotor of the robot's joints must rotate rapidly. Thus, in the present study, ω was set to 1, which is the value at which the servomotor can follow the motion.

In addition, the maximum curvature can be obtained by inverse calculation from the movable range of the joint by using equation (11). Because the movable range of the robot joint is ±90° in this study, the maximum curvature is 13.08. A and ω that satisfy the condition that the curvature is smaller than 13.08 are shown in Figure 10. A and ω in the masked cells are the parameters that can be adopted in actual machine experiments. Note that the masked cells simply denote that they satisfy the movable range based on theoretical calculations. In practical applications, to achieve a sufficient friction between a robot and a pipe, A needs to be adjusted based on the field condition, as will be described in Section 4.2.

ϕ is the initial phase of the helical wave curve. Changing the value of ϕ allows the graph of $\mathrm{sech}(\omega t - \phi)$ to move toward the left and right along the abscissas. In practical applications, to increase the parameter t from 0, it is necessary to move ϕ toward the right by 2π on the abscissas. Therefore, ϕ is set to 2π.

In the next step, the helical wave curve will pass through the entire robot trunk according to the shift control method (Qi et al., 2017). Note that in the present study, only one wave is allowed to pass through a snake robot's trunk at any given time.

Figure 8 Transition of curvature κ depending on parameter A and ω ($r = 0.092$, $n = 0.029$, $\phi = 2\pi$) (see online version for colours)

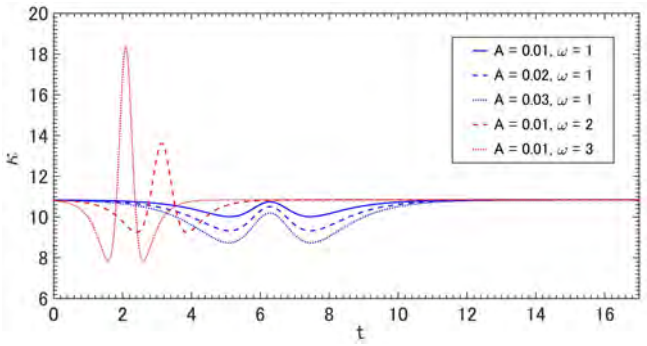

Figure 9 Transition of torsion τ depending on parameter A and ω ($r = 0.092$, $n = 0.029$, $\phi = 2\pi$) (see online version for colours)

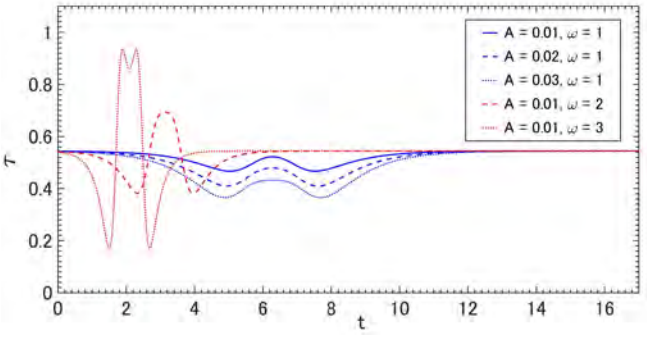

Figure 10 Ranges of A and ω that satisfy the available curvature. (in case of $r = 0.092$, $n = 0.029$ and $\phi = 2\pi$) (see online version for colours)

ω \ A	0	0.01	0.02	0.03	0.04	0.05
1	8.72941	8.97502	9.02929	8.96275	8.82093	8.63345
2	8.72941	11.379	13.1335	14.2696	14.9751	15.3783
3	8.72941	15.3857	19.9739	23.1145	25.232	26.6198
4	8.72941	20.9951	29.5504	35.4972	39.5916	42.3579
5	8.72941	28.2072	41.8631	51.4179	58.054	62.5925

3.2 *Gravity compensation*

When the helical wave curve is applied to a snake robot, the robot is wrapped around a pipe and then a longitudinal wave is generated helps the snake robot lift certain segments of its body off the pipe surface. In the case of a real snake robot, owing to the stiffness of the motor position controller' and mechanical gear gaps, the floating parts of the snake robot deviate from the designed shape under the effect of gravity, as shown in Figure 11(a). Especially, at the start of helical wave propagation, the floating parts act as cantilevers, and gravity strongly influences these parts.

To solve this problem, we propose a method to compensate for the sag of the floating parts. In this method, an extra twist ψ_g is added to the floating parts.

Figure 11 (a) Explanation of phenomenon of robot dropping. (b) Gravity compensation in the part of helical wave propagation (see online version for colours)

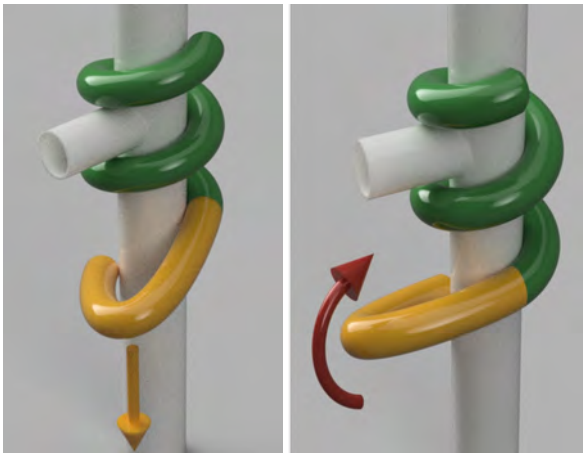

(a) (b)

Notes: The green part denotes the snake robot's trunk attached to the pipe. The yellow part is the part that begins to form a helical wave curve. The yellow arrow shows the direction of gravity. The red arrow shows the direction of twisting by ψ_g.

Thus, the change $\psi(s)$ in equation (5) is expressed as follows:

$$\psi(s) = \int_0^s \tau(s)ds + \psi(0) + \psi_g$$
$$\begin{cases} \psi_g = \tau_g & (0 \le s \le s_c) \\ \psi_g = 0 & (s < s_c) \end{cases} \tag{17}$$

s_c is the point at which the floating parts stop acting as cantilevers and become a helical curve. This compensation is added when the floating parts are cantilevers, which means that the tail of the robot is apart from the pipe. In other parts, ψ_g is set to 0. Determining ψ_g is difficult because it depends on property of the motor controller and mechanical gaps. In this study, the value of ψ_g was determined by trial and error. After compensation, the floating parts are raised against gravity, as shown in Figure 11(b).

4 Experiments

4.1 Snake robot and environments

We verified the proposed method by means of experiments conducted using an actual mechanical snake robot. The system configuration of the snake robot is shown in Figure 12. Software of the snake robot is constructed by Robot Operating System (ROS). We created a package to generate helical wave propagation motion. This package subscribes a command from joystick by an operator and publishes the target angle of each joint as a result of the calculation. The target angle is commanded from the control PC to the motors via RS-485 communication. A slip ring was mounted on the tail of the snake robot, so that the cord does not twist even if the robot executes rolling motion.

Figure 12 Outline of snake robot control system (see online version for colours)

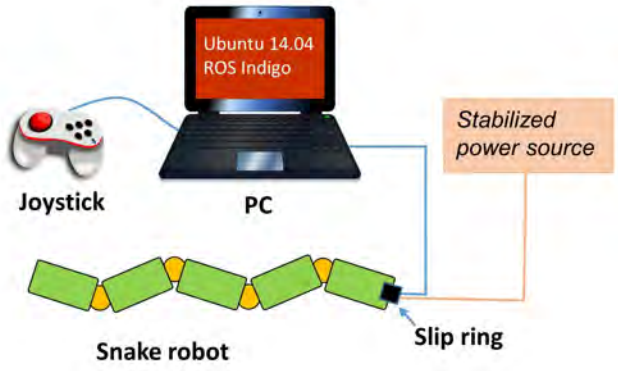

As shown in Figure 13, we constructed a snake robot by connecting Dynamixel XH430R servo motors serially along the pitch and yaw axes alternately. The snake robot comprised 25 joints in total. The distance between each of the axes was 0.060 [m]. The range of motion of the joints was ±90°. The servo motor provided 4.8 [N·m] of torque, and its maximum rotational speed was 37 rpm at 14.8 [V]. The length of one link was 0.060 [m], and the total length of the snake robot was 1.630 [m], which its weight was 3.0 [kg]. To protect the cables of each module, the exterior part of the robot was designed to be mounted on the outside of each servo motor. Moreover, the exterior parts were covered with a sponge rubber ring to achieve greater friction between the snake robot trunk and the pipe. The outer diameter of the sponge rubber rings was 0.070 [m].

The experimental environment is shown in Figure 14. Figure 14(a) shows the test of the available values of parameter A according to Section 3.1. The intersection of the two red lines on the pipe is the start point. The red line along the horizontal direction is defined as the x-axis and that along the vertical direction was defined as the y-axis. The diameter of the PVC pipe was 0.115 [m], and its length was 1.0 [m]. Figure 14(b) shows the test conducted to verify the feasibility of the snake robot passing through a branch on the pipe by using helical wave propagation. The diameter of the PVC pipe was 0.115 [m], length was 2.12 [m], and the diameter of the branch was 0.115 [m]; its length was 1.0 [m]. The pipe was placed vertically in the environment.

4.2 Experiments to determine parameter A

In this section, we conducted a test to verify the effect of parameter A on the values shown in Figure 10.

At first, the head was placed at the start point with the snake robot wrapped around the pipe, as shown in Figure 15(a). Then, the helical wave curve was generated 10 times, and the position of the robot's head was measured. This experiment was repeated 10 times, and the average value was calculated. The result is shown in Figure 16. Note that gravity compensation was not added in this experiment. Thus, the value of ψ_g was always 0. Other parameters were set as follows: $r = 0.087$, $n = 0.026$, $\omega = 1$ and $\phi = 2\pi$.

Figure 13 Overview of laboratory snake robot showing its kinematic configuration (see online version for colours)

Notes: The solid green line is the pitch joint, and the dashed red line is the yaw joint.

Figure 14 Overview of experimental environment (see online version for colours)

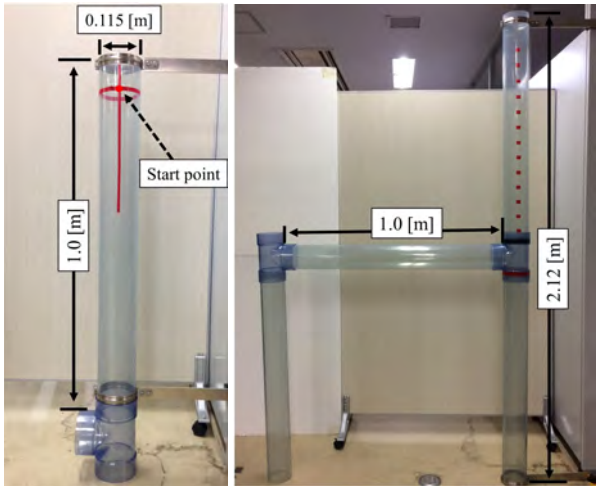

(a) (b)

In the case of $A = 0.01$, movement in the tangential direction along the robot trunk was not observed because the helical wave curve was small. By contrast, because of the twisting compensation (Qi et al., 2017), it generated slight rolling and moved in the binormal direction, as shown in Figure 15(b).

In the case of $A = 0.02$, the helical wave curve was observed, and it was confirmed that the curve moved in the tangential direction to the robot. However, as shown in Figure 15(c), it is observed that the robot slightly slips down owing to the stiffness of the motor position controller and mechanical gear gaps.

In the case of $A = 0.03$, the robot slipped to the bottom of the pipe four times in the experiment, causing those repetitions of the experiment to fail. In the other six repetitions, some slipping was observed, but the robot did not slip to the bottom of the pipe. The position shown in the Figure 15(d) is the average of these six experiment repetitions. In addition, it was found that the displacement along the x-axis increased as A increased.

Figure 15 Experiments to determine parameter A (see online version for colours)

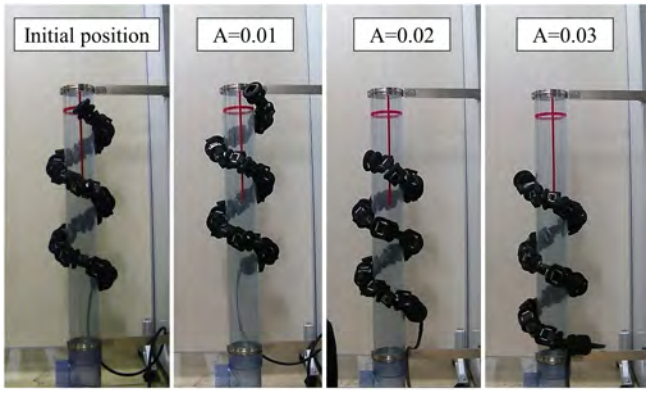

(a) (b) (c) (d)

Figure 16 Experimental results of parameter A (see online version for colours)

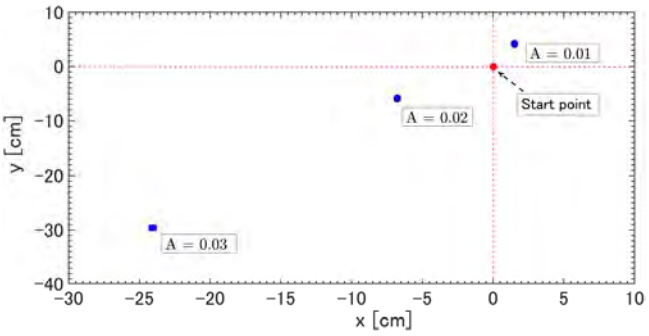

To increase the speed of robot motion, it is preferable to increase the value of A.

As a result, the parameter A was set to 0.02 to achieve the desired helical wave propagation with keeping good frictional condition between the robot and the pipe.

4.3 Experiment of passing through branch point

In this experiment, the feasibility of the robot traversing through a branch on a pipe by means of helical wave propagation was verified.

According to Section 4.1, the radius of the snake robot trunk was $r_r = 0.035$, and the radius of the pipe was $r_p = 0.057$. Thus, $r = 0.092$, and $n = 0.024$. Photographs of the actual machine experiment are shown in Figure 17, where the parameters of the helical wave propagation motion were $r = 0.087$, $n = 0.026$, $A = 0.02$ or 0.03, $\omega = 1$, $\phi = 2\pi$, and $\psi_g = 0.0027$. Because the sponge rubber on the snake robot deformed when the robot wrapped itself around the pipe, it was necessary to set r to a value smaller than the theoretical value. By contrast, the value of n was set to be slightly larger than the theoretical value to avoid friction with the branch. The value of A was set to 0.02 at the beginning to achieve stable helical wave propagation. After the robot's head crossed the branch, A was changed to 0.03 to increase movement speed. This was realised because the branch point supported the robot's body against gravity.

Figure 17 Example of actual machine experiment of helical wave propagation (see online version for colours)

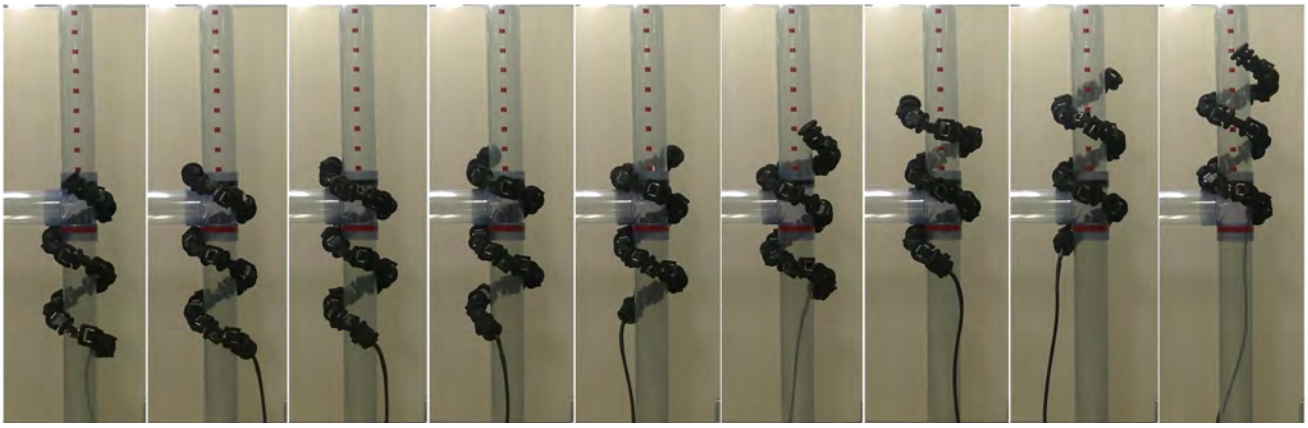

Notes: In this figure, the snake robot passes through the branch point by using helical wave propagation. The figures are separated by intervals of approximately 20 [sec]. The distance between the red marks is 0.065 [m].

Figure 18 Command angle and actual angle of head joint (see online version for colours)

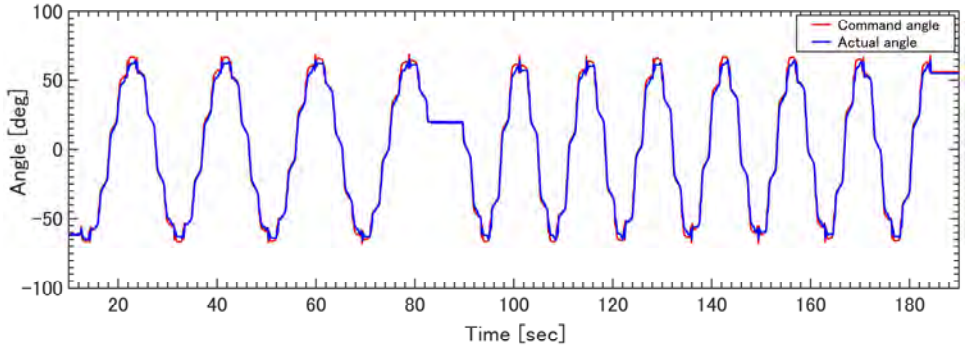

Note: The part surrounded by the broken line is the waiting time at which set the parameter *A* is revised from 0.02 to 0.03.

Figure 19 Partial enlargement from 94[sec] to 108[sec] (see online version for colours)

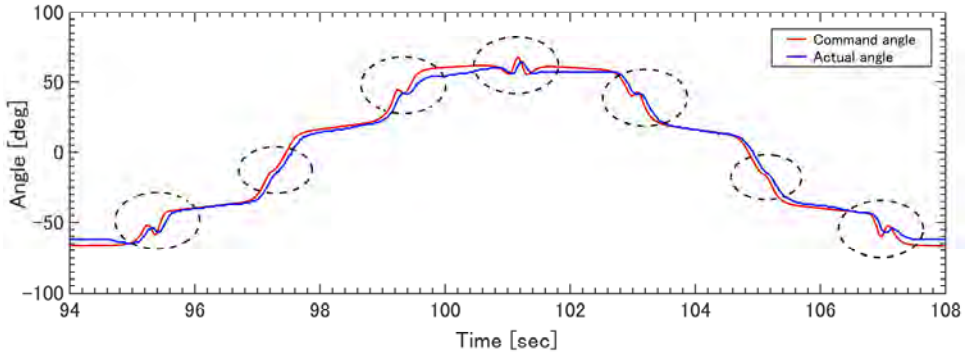

Note: The part surrounded by the broken line is the joint angle at the time of generation of the helical wave curve.

The robot moved from the bottom to the top by using helical wave propagation, and it passed the branch successfully as a result of this new motion. The commanded angle and actual angle of head joint angle are shown in Figure 18. The helical wave propagation was conducted in the part surrounded by the broken line. In Figure 18, the period of change in angle is large because of the twisting compensation described in a previous study (Qi et al., 2017).

5 Conclusions

In this paper, we proposed helical wave propagation motion as a form of motion for a snake robot to overcome branch points on a pipe. Especially, in this paper, we proposed a method to design the parameters of the helical wave curve and to compensate for gravity. A hyperbolic function was adopted to generate a longitudinal wave. The designed helical wave curve in the Cartesian coordinate system was converted into the target angles of each joint of the snake

robot by using the continuous curve model. We conducted experiments by using an ordinary structure of snake robot to verify the behaviour of the proposed helical wave propagation motion with gravity compensation. It was confirmed that by using the helical wave curve propagation, the snake robot could pass through a branch point, which is impossible to achieve by means of conventional helical rolling motion.

In the future work, we will investigate more suitable parameter A and ω by using such as bifurcation theory. Our research group is designing a new snake robot that can sense external pressure on entire links and equipped with an inertial measurement unit on its head and tail. In the future work, we will measure the posture of the robot by using the IMUs installed on the head and tail of the robot and adjust the compensation value ψ_g automatically.

Acknowledgements

This research was funded by ImPACT Program of Council for Science, Technology and Innovation (Cabinet Office, Government of Japan).

References

Baba, T., Kameyama, Y., Kamegawa, T. and Gofuku, A. (2010) 'A snake robot propelling inside of a pipe with helical rolling motion', *Proceedings of the SICE Annual Conference*, Taipei, Taiwan, pp.2319–2325.

Date, H and Takita, Y. (2005) 'Control of 3D snake-like locomotive mechanism based on continuum modeling', *Proceedings of the ASME International Design Engineering Technical Conferences and Computers and Information in Engineering Conference*, Long Beach, California, USA, pp.1351–1359.

Hirose, S. (1993) *Biologically Inspired Robots (Snake-like Locomotor and Manipulator)*, Oxford University Press, Oxford.

Hirose, S. and Yamada, H. (2009) 'Snake-like robots machine design of biologically inspired robots', *IEEE Robotics and Automation Magazine*, Vol. 16, No. 1, pp.88–98.

Kamegawa, T., Harada, T. and Gofuku, A. (2009) 'Realization of cylinder climbing locomotion with helical form by a snake robot with passive wheels', *Proceedings of the IEEE International Conference on Robotics and Automation*, Kobe, Japan, pp.3067–3072.

Kamegawa, T., Matsuno, F. and Chatterjee, R. (2002) 'Proposition of twisting mode of locomotion and GA based motion planning for transition of locomotion modes of 3-dimensional snakelike robot', *Proceedings of the IEEE International Conference on Robotics and Automation*, Washington, DC, USA, Vol. 2, pp.1507–1512.

Lipkin, K., Brown, I., Peck, A. and Choset, H. (2007) 'Differentiable and piecewise differentiable gaits for snake robots', *Proceedings of the IEEE/RSJ International Conference on Intelligent Robots and Systems*, San Diego, CA, USA, pp.1864–1869.

Liu, P., Yu, H. and Cang, S. (2018) 'Geometric analysis-based trajectory planning and control for underactuated capsule systems with viscoelastic property', *Transactions of the Institute of Measurement and Control*, Vol. 40, No. 7, pp.2416–2427.

Mori, M. and Hirose, S. (2001) 'Development of active cord mechanism ACM-R3 with agile 3D mobility', *Proceedings of the IEEE/RSJ International Conference on Intelligent Robots and Systems*, Maui, HI, USA, Vol. 3, pp.1552–1557.

Qi, W., Kamegawa, T. and Gofuku, A. (2017) 'Helical wave propagate motion on a vertical pipe with a branch for a snake robot', *Proceedings of the International Conference on Swarm Behavior and Bio-Inspired Robotics*, Kyoto, Japan, pp.105–112.

Rollinson, D. and Choset, H. (2016) 'Pipe network locomotion with a snake robot', *Journal of Field Robotics*, Vol. 33, No. 3, pp.322–336.

Yamada, H. and Hirose, S. (2006) 'Study on the 3D shape of active cord mechanism', *Proceedings of the IEEE International Conference on Robotics and Automation*, Orlando, FL, USA, pp.2890–2895.

Yamada, H. and Hirose, S. (2010) 'Approximations to continuous curves of active cord mechanism made of arc-shaped joints or double joints', *Proceedings of the IEEE International Conference on Robotics and Automation*, Anchorage, Alaska, USA, pp.703–708.